5

An HI absorption study of the Warm Neutral Medium

If you saw a heat wave, would you wave back?

—Steven Wright

Summary and the main results of chapter 5

Of all the phases in the ISM, the Warm Neutral Medium (WNM) remains the least understood. The spin temperature of the WNM and its filling factor are important parameters with implications on the models of the ISM, but only two measurements of HI absorption from the WNM exist till date and they are very recent. We have carried out a very high sensitive HI 21cm-line absorption study using the Westerbork Synthesis Radio Telescope, towards 5 extragalactic radio continuum sources. This chapter discuss the results obtained:

- ***We have detected HI absorption in the Warm Neutral Medium of the Galaxy towards 3 directions. The measured HI optical depth is in the range 0.0014 to 0.004.***
- ***The estimated spin temperature varies from $\sim$2500K $-$ 1400 K. We obtained an upper limit of $\sim$ 5200K towards the fourth line of sight.***
- ***The spin temperatures derived from our observations agree with the predictions of the two phase models of the ISM***
- ***We have also detected HI absorption in the high velocity gas in the Outer Arm Complex towards one line of sight. The inferred spin temperature is $\sim$ 450K.***
- ***In addition, we have also detected an unusual HI absorption feature ($\tau \sim$ 0.0009), the position and width of which seem to be correlated to a low T_B ($\sim$ 0.1K) wide ($\sigma_v \sim$ 66 km s^{-1}) HI emission feature in the Leiden Dwingeloo Survey, which are known as the large velocity dispersion (LVD) HI gas.***

5.1 INTRODUCTION

5.1.1 Background

The early HI 21cm line absorption and emission studies led to the emergence of a global picture of the Interstellar Medium (Clark, Radhakrishnan & Wilson, 1962; Clark, 1965; Radhakrishnan et al., 1972). These and later studies have established that the neutral ISM in the Galaxy consists of cool dense clouds (the Cold Neutral Medium or CNM) in pressure equilibrium with a warmer Intercloud medium (Warm Neutral Medium or WNM). The spin temperature of the cold clouds which constitute the CNM was estimated to be around 80 K and that of the WNM is 8000 K. The basic data that differentiate between the two phases is shown in Fig 2.1 (From Radhakrishnan et al., 1972). This shows both emission and absorption spectra. The narrow emission components which have absorption counterparts arise in the cold neutral medium (CNM). The broad emission components which do not have absorption counterparts arise in the WNM. Due to the higher temperature of the WNM, assuming the HI spin temperature also to be high, measuring HI absorption from the WNM is difficult since for the HI line,

$$\tau_{HI} \propto \frac{N_{HI}}{T_S} \tag{5.1}$$

Where τ_{HI} is the optical depth of the HI absorption line, T_S is the spin temperature and N_{HI} is the HI column density, obtained from the HI emission line brightness temperature, given by

$$N_{HI} = 1.823 \times 10^{18} \int T_B dV \quad cm^{-2} \tag{5.2}$$

In the above equation, v, the velocity is in km s^{-1}.

The early HI studies of the Galactic Interstellar medium provided only HI emission signature of the WNM. The half power velocity width of the WNM emission features are of the order of $\sim$17 km s^{-1} and above, whereas the narrow HI lines from the CNM are usually a few km s^{-1} wide.

The observational evidence for the two components in the ISM was supported by theoretical models in which low energy cosmic rays supply the energy for the heating of the Interstellar gas, while radiation from excited levels of heavy elements and ions are responsible for cooling it (Field, Goldsmith & Habing, 1969). A comprehensive review of the heating and cooling of HI regions is given by Dalgarno & McCray (1972). Later theories of the ISM emphasized the importance of supernovae which continuously perturb the gas and produce large connected volumes of very hot (T $\sim 10^6$) rarefied gas with a high filling factor (Cox & Smith, 1974; McKee & Ostriker, 1977). In these theories, the WNM is not pervasive, but surrounds the colder clouds.

The phases of the ISM are thought to be in pressure equilibrium, although the relative filling factors of the different phases remain uncertain and may vary with

position in the Galaxy (Braun & Walterbos, 1992). The most detailed analysis of the equilibrium state of neutral hydrogen in the ISM was carried out by Wolfire et al. (1995). The primary heating mechanism is photo electric emission from dust grains, while cooling is dominated by fine structure lines from heavy elements in cold regions and by hydrogen recombination lines in warmer regions.

Assuming pressure equilibrium, an estimate of the kinetic temperature of the WNM can be used to calculate its volume density. The HI emission measurements, on the other hand, provide an estimate for the average column density along the line of sight. The spin temperature of the WNM is an important parameter with implications for models of the Interstellar medium. Recall that all the earlier observations detected only HI emission from the WNM. Till very recently, there were no successful absorption measurements. To verify the predictions of various theoretical models, one need to have an estimate of temperature of the gas. HI observations can yield the spin temperature **only if both the emission and absorption data are available**, because the spin temperature is given by

$$T_S = \frac{T_B}{1 - e^{-\tau}} \tag{5.3}$$

For a multi phase medium, however, the measured spin temperature is the column density weighted harmonic mean of the temperatures of different phases.

5.1.2 The measurable Spin temperature of HI gas

Before proceeding further, we would like to elaborate on equation 5.3. For a given line of sight, with a number of regions 1,2,3..., with individual optical depths τ_1, τ_2, τ_3, etc., and spin temperatures T_1, T_2, T_3, etc. respectively, the observed HI brightness temperature is given by

$$T_B = T_1(1 - e^{-\tau_1}) + T_2(1 - e^{-\tau_2}) + T_3(1 - e^{-\tau_3}) + ... \tag{5.4}$$

Under the assumption that each of the individual optical depths, as well as their sum is much less than unity, each $T_i(1 - \mathrm{e}^{-\tau_i})$ in the above equation can be approximated as $T_i\tau_i$.

The measured HI absorption is given by

$$(1 - e^{\tau}) = 1 - e^{(\tau_1+\tau_2+\tau_3+...)} \tag{5.5}$$

Using equations 5.4 and 5.5, and assuming the optically thin case, one can rewrite equation 5.3 as

$$T_S = \frac{T_1\tau_1 + T_2\tau_2 + T_3\tau_3 + ...}{\tau_1 + \tau_2 + \tau_3 + ...} \tag{5.6}$$

Thus the measured spin temperature is the opacity weighted mean.

However, this is valid only for low optical depth for each individual features. Assuming the spin temperature to be either $\sim 10^2$ or $\sim 10^4$ (for the CNM & WNM - as predicted by the various models), we find that only if each of the individual HI line brightness temperatures ($T_i(1 - e^{-\tau_i})$) and hence the column densities (equation 5.2)are all roughly the same, we can say that the measured spin temperature is the harmonic mean.

From the definition of the HI optical depth,

$$\tau \propto \frac{\int n_{HI} dl}{T_S} \tag{5.7}$$

Therefore, the cold components dominate the measured optical depth. Hence, the estimated spin temperature will provide only a lower limit for the cold component. If one can measure the optical depth of the WNM, the mean spin temperature gives only a weak lower limit to the actual spin temperature (Braun & Walterbos, 1992).

In an HI absorption search of the WNM, it is of prime importance to choose lines of sight that contain minimum number of cold clouds. For a more accurate estimate of the spin temperature of the WNM, one need to have velocity ranges in the spectra where no HI features from the CNM is present.

5.1.3 The spin temperature of the WNM

The spin temperature of Interstellar HI gas is determined by a number of factors. To begin with, the gas is swamped in the cosmic microwave background radiation (CMBR). If this is the only exciting mechanism, the spin temperature of the gas would be equivalent to the black body temperature of the background radiation, which is 3K in the local universe. The 21cm-line would have been unobservable, except for absorption lines towards radio continuum sources where the continuum brightness temperature of the background source is different from that of the CMBR. In a more general sense, one can state that the ambient radio continuum flux at the wavelength of the 21cm-line is a factor which affects the spin temperature of the line. There are two other excitation mechanisms which influence the spin temperature: Collisions and Lyα radiation. Both these factors and their relevance in the case of the warm neutral medium are examined in detail below.

It is usually believed that the spin temperature of the HI gas is equal to the physical (kinetic) temperature of the gas. Much of our basic understanding of the phases of the ISM is from the measurements of the HI spin temperature. *An important factor that can equalize the spin temperature and the kinetic temperature is the dominance of collisional excitation of the 21cm line.* $i.e.$ the number of density of the H atoms are large enough so that collisions are important. In such a situation, the thermal motion of the atoms (and thereby collisions) is the dominant factor that excite the hyperfine levels. Therefore, spin temperature is close to the kinetic (physical) temperature of the gas. For the case of cold HI clouds, where the number density of HI atoms is

$\sim$ 10 cm^{-3}, the collisions determine the spin temperature of the gas. For the CNM, measured value of HI spin temperature averages to $\sim$ 80K, close to the expected kinetic temperature of the gas, inferred from line widths and from the conditions for pressure equilibrium with the warmer Intercloud medium. However, while dealing with the Intercloud medium, where the temperature is two orders of magnitude above that of cold clouds (T$_k$ $\sim$ 8000K), pressure equilibrium requires the number density to be lower by the same factor. Hence, collisions can no longer thermalize the 21cm line transition. Therefore spin temperature measurements of the WNM can imply lower kinetic temperatures in a range, say 1000-5000K or so, where the gas is unstable in multiphase models (McKee and Ostriker, 1977; Wolfire et al., 1995).

An often ignored mechanism for the excitation of HI is the Ly-α radiation field. Excitation by the Ly-α photons dominates hyperfine excitation locally around individual stars. Solar Ly-α radiation is important for the local HI gas within $\sim$1000 AU of the sun (Brasken & Kyrölä, 1998). This range of influence is much larger for an O or B star. In the Interstellar medium, the excitation of hyperfine line by the scattered Ly-α radiation is known as the Wouthuysen-Field mechanism (Wouthuysen, 1952; Field, 1958 & 1959). Since the oscillator strength for the Ly-α transition is very high, the optical depth for Ly-α photons in an HI cloud is very large ($\sim$10^6). A Ly-α photon undergoes repeated absorption and re-emission as it traverse an HI cloud. Emission/absorption of a Ly-α photon involves transition to/from the electronic ground state in an H atom. The repeated absorption and re-emission of these photons in an HI cloud and the recoil of each emitting atom, coupled to the random motions of the atoms results in Ly-α photons carrying information of the gas motion in their wavelength distribution. Hence, the Ly-α photons tend to impart the influence of the random motions of the gas to the hyperfine transition and the corresponding excitation temperature. Therefore, the ambient Ly-α radiation field can couple the kinetic motions of the gas atoms to the spin temperature, thereby boosting the spin temperature towards the physical temperature of the gas. This can play an important role in low density HI regions like the WNM, where the number density of the HI gas is not sufficient for collisional excitation to be dominant for the 21cm line. The number of Ly-α photons threading the Interstellar medium is larger near star forming regions and OB associations. Therefore, the spin temperature of the WNM can be expected to span a large range.

5.1.4 A Note on the HI line widths

It is usually expected that the absorption line widths are always narrower than the emission lines. This apparent difference can be explained using equation 5.3. The terms (1 – e$^{-\tau}$) and T$_B$ has different sensitivities to variations of the spin temperature of the gas along the line of sight. However, this difference is obvious only for larger optical depths as in the case of the cold clouds that constitute the CNM. For $\tau << 1$, which is expected for the WNM, equation 5.3 can be rewritten as

$$T_S = \frac{T_B}{\tau} \tag{5.8}$$

Therefore the emission and absorption line widths are expected to be identical for the very low optical depth features, as in the case of the WNM.

5.1.5 The Filling factor of the WNM

Assuming pressure equilibrium, an estimate of kinetic temperature of the WNM (Spin temperature is obtained from the HI absorption and emission measurements) leads to an estimate of the number density of the WNM (equation 5.9). The corresponding values for the cold clouds which constitute the CNM is well known.

$$n_{CNM} T_{CNM} = n_{WNM} T_{WNM} \tag{5.9}$$

The HI emission measurements, on the other hand, provide an estimate of the average column density, N_{HI} along the line of sight. If the pathlength sampled is known, an average value of the volume density of the WNM, $\langle n_{WNM} \rangle$ can be obtained from this. Using the number density of the WNM, n_{WNM} and its average number density, one can estimate the volume filling factor using the following relation.

$$f = \frac{\langle n_{WNM} \rangle}{n_{WNM}} \tag{5.10}$$

5.1.6 Existing HI absorption measurements of the WNM

As we mentioned earlier, of all the phases in the ISM, the WNM remains the least well understood. Although HI emission from the WNM is detected easily in almost every direction in the sky, measuring the HI absorption from the WNM is difficult, due to its higher temperature ($\tau_{HI} \propto N_{HI}/T_S$). There has been several attempts to measure the optical depth of the WNM. Mebold & Hills (1975) estimated an optical depth for the WNM based on the lack of HI emission in their measurements using the Effelsberg 100m telescope. They estimated the spin temperature of the WNM to be in the range 3000 to 8000 K, in different velocity ranges towards Cygnus A. All other attempts gave only upper limits for absorption from WNM and hence lower limits for the spin temperature.

Recently, Carilli, Dwarakanath & Goss (1998) detected HI absorption from the WNM towards Cygnus A at LSR velocities of –40 km s^{-1} and –70 km s^{-1}. These two velocity ranges were previously identified as being relatively free of cold absorbing clouds. The measured optical depth for the WNM along this line of sight is $(8.9 \pm 1.9) \times 10^{-4}$ at –70 km s^{-1} and $(8.5 \pm 2.0) \times 10^{-4}$ at –40 km s^{-1}, with corresponding spin temperatures of 6000 ± 1700 and 4800 ± 1600 K respectively. The volume filling factor for the WNM appears to be fairly high and is ~ 0.4.

The detection of WNM absorption towards Cygnus A was followed by another detection by Dwarakanath, Carilli & Goss (2002). One of the difficulties encountered in estimating the spin temperature of the WNM towards Cygnus A is the plethora of absorption lines arising from the CNM. The absorption due to the WNM is apparent only at those velocities which fall in between the velocity ranges covered by the two spiral arms along this line of sight, where the cold gas is absent. In order to avoid this, Dwarakanath, Carilli & Goss (2002) measured HI absorption towards sources at moderate to high latitudes, where HI absorption from CNM is less as compared to a sight line through the Galactic plane. The advantage of making HI absorption measurements toward directions relatively free of the CNM is that one will be able to actually detect the weak HI absorption line arising in the WNM, instead of estimating the optical depth of the WNM in the CNM-free regions (as was done in the case of Cygnus A). Indeed, the results from this observation proved this argument (Dwarakanath, Carilli & Goss, 2002) and HI absorption was detected from the WNM towards 3C147. The estimated spin temperature of the WNM from this observation is 4500 ± 500 K. However, towards the other three sources located at higher latitudes, the pathlength traversed through the Galactic ISM was smaller and the absorption arising in the WNM was below the sensitivity limits. It was clear from this study that we need to look for sources at moderate Galactic latitudes to detect HI absorption arising from the WNM. However, one should also refrain from observing at such low latitudes where the forest of narrow HI absorption features due to the cold gas mask the shallow HI absorption from the WNM.

5.1.7 Motivations for the present Study

Absorption measurements towards several directions in the Galaxy will result in a more accurate, global estimate for the optical depth and thereby spin temperature of the WNM. An estimate of the spin temperature of the WNM obtained from the HI absorption measurement along the given line of sight leads to an estimate of the volume density n_{WNM} of the WNM, assuming pressure equilibrium. The HI emission measurements, on the other hand give an estimate of the average column density, N_{HI} along the line of sight. An average value of the volume density of the WNM, $\langle n_{WNM} \rangle$ can be obtained from this if the length along the line of sight is known. A combination of the actual volume density and the average volume density leads to the filling factor of the WNM. The filling factor is an important number but is poorly determined. Its variation with the Galactic latitude and its possible relation to the location of the spiral arms of the Galaxy are of vital importance in understanding the ISM.

In this context, what is required now is a search for WNM absorption at moderate latitudes and towards lines of sight that sample a range of Galactic longitudes. This set of observations will be a powerful tool in exploring the possible variations in the properties of the WNM. Combining the results of this proposed observations with those from the earlier observations would help us derive important information

regarding the physical parameters of the WNM.

These observations require a very high spectral dynamic range, because here the search is for an optical depth of $\sim 10^{-3}$ among the deep, often optically thick features arising from the cold clouds. Spectral dynamic range of 1 part in 7,500 or better is required and the only instrument which can provide bandpass stability to reach these levels in reasonable integration time is the Westerbork Synthesis Radio Telescope.

5.2 SOURCE SELECTION

We have chosen a list of 5 extragalactic radio continuum sources from the VLA calibrator manual. The selection criteria was that the Galactic latitude of the source should be less than $\sim 15^o$ and the 20cm flux density > 5Jy and the sources should be at an observable declination for the WSRT. An additional criterion was the number of spectral features arising from the CNM should be minimum. The HI emission profile toward each of these 5 sources (From the Leiden-Dwingeloo Survey of Galactic neutral hydrogen) shows less than 8 narrow components. The wide HI emission feature arising from the WNM is prominent in all these directions, with a mean value, $T_B \sim$ 6.0 K. The existing HI absorption data towards all these sources (Dickey et al., 1983; Mebold et al., 1981) indicates only narrow absorption features from the CNM since the WNM absorption is at levels below the sensitivity limits of these surveys.

The most detailed analysis of the equilibrium state of neutral hydrogen in the Interstellar medium, carried out by Wolfire et al., 1995, estimates the temperature of WNM to be $\sim$ 5500 K to 8700 K. The present set of observations are sensitive to detect HI absorption from such a gas. In case of non-detections, the 3σ level of HI optical depth achieved in this set of observations would demand a lower limit for the spin temperature of WNM to be up to to 13,500 K. This limit is so high as to call for a revision of the existing models of the ISM.

5.3 OBSERVATIONS & DATA REDUCTION

The Observations were carried out using the Westerbork Synthesis Radio Telescope (WSRT) during the period July-October, 2001. We employed frequency switching on the respective sources to estimate the bandpasses. Each source was be observed for 2×12 hours - 12 hours 'ON' and 12 hours 'OFF'. Each scan on the source at the line frequency was followed as well as preceded by the bandpass calibration scans, where the observing band was shifted by one full bandwidth above and below the line frequency. We used a bandwidth of 1.25 MHz, 256 channels and hanning smoothed to a velocity resolution of 2.1 km s^{-1}. With this observing setup, the expected rms noise per channel is $\sim$ 1.3 mJy/beam over $\sim$ 12 hours. Table 5.1 summarizes the

Table 5.1 The Observational Setup.

Telescope	WSRT
System temperature	$\sim$ 26 K
Number of antennas	14
Base band used	1.25 MHz
Number of channels	256
Velocity resolution	2.1 km s^{-1} (Hann. smoothed)
On source integration time	$\sim$ 12 Hours/source

observing setup.

The analysis of the data was carried out using the Astronomical Image Processing System (AIPS) developed by the National Radio Astronomy Observatory. Continuum subtraction was carried out by fitting a linear baseline to the line free channels in the uv data and subtracting the best fit continuum from all the channels (AIPS task - UVLIN). The final line cubes, after self calibration and CLEAN were made with a lower uv range cutoff which varied from 1.0 kλ to 1.5 kλ, depending on the direction. This is required to prevent the contamination of the absorption spectra by the HI emission entering the synthesized beam. The bandpass calibration scans, with frequency switched above the observing band were applied on the scans where the frequency was switched to below the observing band to convince ourselves that the residual bandpass errors are lower than the HI optical depth variations in the spectrum.

In order to study the individual HI absorption components, multiple Gaussian profiles were fitted to the absorption line spectra using the Groningen Image Processing System (GIPSY). Apart from the new HI absorption measurements with the WSRT, we have extracted the HI emission profiles towards these lines of sight from the Leiden-Dwingeloo sky survey (Hartmann & Burton, 1996). These profiles were also fitted with multiple Gaussian components using GIPSY. Multiple gaussian components were fitted simultaneously to each of the profiles with the minimum number of gaussian components for a reduced chi-square value near 1. In those cases where the central velocities of the HI absorption and emission features agree within the errors, we assume the emission and absorption to arise in the same feature. The list of observed sources are listed in table: 5.2. One of the program sources, J2202+422, happened to be the BLLAC. The measured continuum flux density for this source is 2.0 Jy, though the VLA calibrator manual gives a value of 6.1 Jy. This source is known for intrinsic variations in the flux density.

Table 5.2 The Observed sources.

	Source	S_{20cm} (Jy)	l (deg)	b (deg)	Synthesized beam (FWHM in arc sec)	τ_{rms}
1.	J0502+252	4.2	177.73	–09.91	40.7×18.4 @+0.4	3.7×10^{-4}
2.	J0521+166	7.5	187.41	–11.34	57.1×13.1 @+0.3	1.9×10^{-4}
3.	J2038+513	3.8	088.81	+06.04	17.9×14.5 @00.0	3.8×10^{-4}
4.	J2052+365	4.3	078.86	–05.12	22.9×14.5 @–0.2	2.0×10^{-4}
5.	J2202+422	2.0	092.59	–10.44	21.6×14.9 @–0.1	6.0×10^{-4}

5.4 RESULTS AND DISCUSSION

We have measured the HI absorption towards 5 bright radio continuum sources located at Galactic latitude $|b| < 15^{\circ}$. We have extracted HI emission profiles towards these directions from the Leiden-Dwingeloo sky survey. The emission and absorption data were combined to give the spin temperature of the gas in the associated HI clouds. As mentioned in Chapter 3, The Leiden-Dwingeloo survey used the 25 meter Dwingeloo telescope to map the sky in HI emission. *The half power beam width of the Dwingeloo telescope is* $\sim 36^{'}$*, as compared to the synthesized beam width of few arc seconds for the WSRT*. Hence, there are obvious uncertainties in the detailed correspondence between the HI emission and absorption spectra. However, since the Intercloud Medium is likely to be widespread, the errors in the derived spin temperatures are expected small.

The first detection of HI absorption in the WNM (Carilli et al, 1998) was a report of very low, HI optical depth in the two CNM free velocity ranges towards Cygnus A. Subsequently Dwarakanath et al. (2002) have detected discrete gaussian absorption features arising in the Intercloud Medium.

We have detected HI absorption in the warm neutral medium towards three out of the five program sources. **The derived spin temperatures are in the range $\sim$1500K to 2500K**. All these values are low compared to the kinetic temperatures $\sim$8000 K of the WNM predicted by various theoretical models. *The HI spin temperature of the Intercloud medium is expected to be close to its kinetic temperature through the process of resonant scattering of ambient Ly-α photons* (Field, 1958). The value of Ly-α radiation field in the Interstellar space is not known and it is expected to vary with direction depending on the proximity to hot stars and star forming regions. Liszt (2001) has discussed this problem in detail. He relates the spin temperature and kinetic temperature with number density of H-nuclei, the gas pressure of the Interstellar medium and the fraction of Ly-α flux threading the ISM. In the light of his results,

we discuss below each of our detections. We wish to mention that recent Arecibo observations indicate that a significant fraction of neutral gas in the Galactic ISM may be in the unstable phase with kinetic temperatures in the range 500K to 5000K (Heiles & Troland, 2000; Heiles, 2001).

In the following subsections, we briefly explain the spectra, the discrete HI absorption and emission features derived from it, followed by a brief discussion of the results obtained.

5.4.1 J0502+252

The HI spectra towards this source is shown in figure 5.1. Figure 5.1a displays the HI emission profile from the Leiden-Dwingeloo survey and the HI optical depth profile from our observations. Also shown is the approximate variation of the radial component of Galactic differential rotation along the line of sight as a function of distance (the scale on the left side), and as a function of vertical height (the scale along the right side). Figure 5.1b shows the HI optical depth profile, with a magnified y-axis to show the low optical depth features. The dotted line are the fitted gaussian models for the low optical depth features. The bottom of this figure shows the residuals, after the gaussian model is subtracted from the observed HI optical depth profile. We have actually fitted gaussians to **all** the absorption features. But for the sake of clarity, we have only shown those gaussians that are relevant to the inference of very low and very wide absorptions (this is true for the subsequent figures too).

This source has the Galactic co-ordinates, l = 177.73 deg. and b = –9.91 deg., almost in the direction of the Galactic Anticenter. *The cold gas seen in HI emission as well as absorption*, is found to be in two distinct velocity ranges: $\sim$0 – 10 km s^{-1} and $\sim$–30 km s^{-1} (See Table 5.4.1). Those features near –30 km s^{-1}, presumably related to the Perseus spiral arm of the Galaxy, and those near zero LSR velocity originate in the local spiral arm. The derived spin temperatures of all the narrow HI absorption features are below 100K.

5.4.1.1 Low optical depth features We now turn to figure 5.1.b. The sharp and narrow feature at –11.8 km s^{-1}, with an FWHM of 4 km s^{-1}, has a peak optical depth of 0.0073 (See table 5.3). There is no corresponding HI emission feature seen in the Leiden-Dwingeloo survey data. The width of this feature $\sim$ 4 km s^{-1} is similar to the cold diffuse Interstellar clouds. If this feature is attributed to the cold neutral phase, with a typical kinetic temperature of 100K, then the implied HI column density $N_{HI} \sim 4.3 \times 10^{18}$ cm^{-2}. Remarkably, this is two orders of magnitude smaller than the column density of the typical clouds.

There is, in addition a wider HI absorption feature (FWHM $\sim$ 60 km s^{-1}) with a corresponding HI emission feature of similar width (FWHM $\sim$ 42 km s^{-1}). **We**

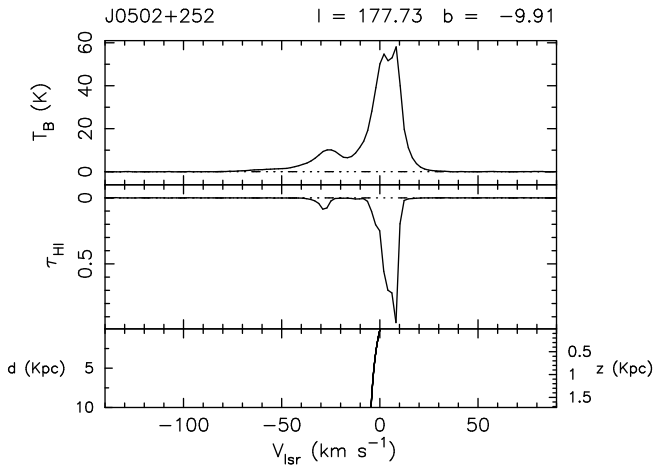

(a)

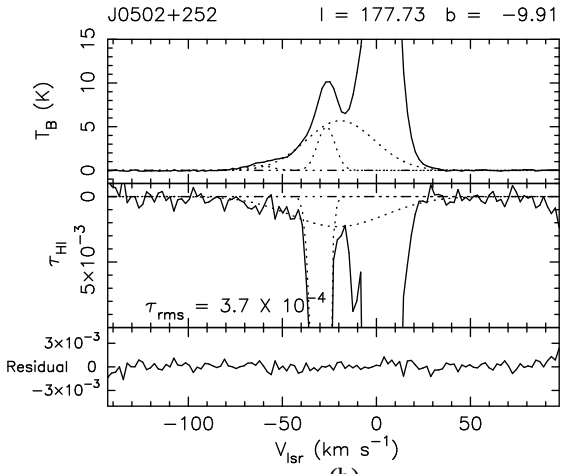

(b)

Fig. 5.1 The HI optical depth spectra from the WSRT towards the source J0502+252 along with the HI brightness temperature profile towards the same line of sight from the Leiden-Dwingeloo survey and the approximate variation of radial component of Galactic differential rotation along the line of sight, as a function of distance (the scale along the left side) and as a function of vertical height (scale on the right side). Figure(b) shows the same HI optical depth and emission profiles, except that the y-axis is magnified to show the very low optical depth features and their HI emission counterparts. The dotted lines are the fitted gaussian models for these features and the lower panel shows the residual in the optical depth spectrum after subtracting the Gaussian model from the observed profile.

Table 5.3 The discrete HI absorption & emission components, identified from the profiles towards the source J0502+252. Column 7 lists the HI column density derived from the HI emission data and column 8 shows the calculated spin temperature.

Absorption (WSRT)			**Emission** (LDS)				
τ_{HI}	V_{lsr} (km s^{-1})	FWHM (km s^{-1})	T_B (K)	V_{lsr} (km s^{-1})	FWHM (km s^{-1})	N_{HI} $\times 10^{20}$ (cm^{-2})	T_S (K)
0.98(0.02)	+7.66(0.03)	3.31(0.04)	27.5(0.5)	+8.55(0.02)	4.43(0.05)	2.4	28(1)
0.03(0.01)	+6(2)	12(2)	—	—	—	—	
0.68(0.01)	+3.38(0.01)	3.6(0.2)	35(1)	+3.24(0.05)	16.7(0.3)	11.0	51(3)
0.20(0.02)	–1.3(0.2)	5.5(0.4)	17(1)	+1.63(0.06)	7.4(0.2)	25.0	85(15)
0.0073(0.0006)	–11.8(0.2)	4.0(0.5)	—	—	—	—	
0.071(0.003)	–28.03(0.02)	4.1(0.1)	5.0(0.1)	–26.6(0.1)	10.8(0.4)	1.1	70(5)
0.025(0.002)	–30.6(0.3)	8.2(0.3)	—	—	—	—	
0.0023(0.0003)	–20(3)	59(5)	5.7(0.2)	–19.2(0.9)	42(1)	4.7	2478(470)

identify this shallow absorption feature to the HI gas in the Intercloud medium. The derived spin temperature ($T_s = T_B/(1 - e^{-\tau})$) **of this feature is $\sim$2500 K**.

As discussed in section 5.1.3, the most important factor that influences the spin temperature is the Lyα radiation field. Resonant scattering of Lyα photons by hydrogen atoms can raise the spin temperature towards the kinetic temperature, even in the absence of collisions. Liszt (2001) has discussed the variation of spin and kinetic temperatures with Lyα radiation field, the number density of the atoms and the interstellar gas pressure for the various existing models of the ISM. Following the results by Liszt, *the spin temperature $\sim$2500K obtained from our observations would imply a kinetic temperature of $\sim$8000K and a number density of 0.2cm^{-3} for the absorbing gas* if the fraction of Ly-α flux from early type stars that permeates the interstellar medium is 0.0001 or below (Fig. 5 in Liszt, 2001). For any larger value for this fraction of Ly-α flux, the spin temperature should be even higher (and closer to the kinetic temperature), to maintain the pressure equilibrium and a stable phase for the WNM. The spin temperature derived from our study is not in agreement with the values predicted by McKee & Ostriker (1977). Their 3 phase model predicts a spin temperature of $\sim$5500K or above for the WNM, even with no contribution from the Ly-α radiation field.

Recall that the narrow HI absorption/emission features are seen at two distinct velocity ranges, corresponding to the two spiral arms - the local arm and the Perseus arm. The Warm gas seen in absorption, on the other hand, is centered at $\sim$–20 km s^{-1}, almost midway between the local and the Perseus arm in the velocity space. The width of this feature is $\sim$ 59 km s^{-1}. If this width has a kinematical origin, then using the model of Galactic rotation by Brand & Blitz (1996), we obtain the extent of this feature along the line of sight to be $\sim$ 4.5 Kpc. The Perseus arm is at a distance of $\sim$ 1.5 – 2 Kpc from us. Therefore, one cannot rule out the possibility that what we measure is the optical depth of the Intercloud medium extending beyond the Perseus arm.

5.4.2 J0521+166

The HI spectra towards this source is shown in figure 5.2. As in the previous case, Figure 5.2a displays the HI emission profile from the Leiden-Dwingeloo survey and the HI optical depth profile from our observations, along with the approximate variation of the radial component of Galactic differential rotation along the line of sight, as a function of distance (the scale on the left side) and as a function of vertical height (the scale along the right side). Figure 5.2b shows the HI optical depth profile, with a magnified y-axis to show the low optical depth features. The dotted line are the fitted gaussian models for the low optical depth features. The second panel in this figure shows the residuals, after the gaussian model is subtracted from the observed HI optical depth profile.

This source is towards l = 187.4° and b = –11°, again close to the anticenter direction. As in the previous case, narrow HI absorption features clearly show two different groups in terms of their velocities (Table 5.4). One originating in the local spiral arm and the other one in the Perseus arm.

5.4.2.1 Low optical depth features The rms optical depth level in this dataset is 1.9×10^{-4}. Fig. 5.2.b seems to indicate a range of velocities starting from ∼–100 km s^{-1} where the optical depth level is more than 3σ above the rms level. Notice the shallow HI emission feature and the corresponding HI absorption in the same velocity range. This shallow HI emission feature has an FWHM of ∼150 km s^{-1} and a peak line brightness temperature of ∼0.1K (Table 5.4). Such features are known as the **large velocity dispersion gas** (LVD), and its nature has been studied by Kalberla et al (1998) and others. Though Kalberla et al (1998) averaged spectra over several degrees to detect the LVD HI emission features, one can expect these features to show up in single pointing spectra also (Kalberla, private communication). Hence, assuming the absorption and emission to arise in the same gas, we obtain the spin temperature $T_S \sim 100$ K. The bandwidth used in the present observations (1.25MHz = ∼ 265 km s^{-1}) has barely managed to recover this unusually wide HI absorption feature. The residual bandpass errors for this data is at a level of one part in 6000 ($<2.0 \times 10^{-4}$ in τ_{HI}) which is much below the peak optical depth of $\sim 10^{-3}$ from the LVD feature. **If confirmed, this will be the first evidence for HI absorption from the large velocity dispersion gas.**

The Gaussian fit to the HI emission profile indicates the presence of a discrete feature centered at ∼–11 km s^{-1}, with a peak T_B ∼5K and FWHM ∼48 km s^{-1}. No corresponding HI absorption was detected from our observations. *The derived lower limit for the spin temperature is ∼5300K*. It is rather surprising that about 12° away, towards the source J0502+252 we obtained a spin temperature of ∼2500K for the Intercloud medium, whereas in this case T_S is above 5300K. This line of sight is passing through the Eridanus supershell. The shell encircles hot, x-ray emitting gas, which is undoubtedly the result of energy released by massive stars. There is a noted absence of radio continuum emission within this shell, which confirms the idea that the energy comes from stellar winds, rather than supernovae. The presence of massive stars would mean an enhanced flux of Ly-α photons. Therefore, we conclude that for this direction, the spin temperature of the WNM is close to the kinetic temperature. **This may be the first evidence for the correlation between spin temperature of the Intercloud medium and the ambient Lyα radiation field.**

5.4.3 J2038+513

Figure 5.3.a shows the HI emission and absorption profiles towards this source and Fig. 5.3.b shows the low optical depth features in the HI absorption profile. This source is located in the first Galactic quadrant with co-ordinates (88.81°, +6.04°). The HI emission profile consists of 9 discrete Gaussian components. HI absorption

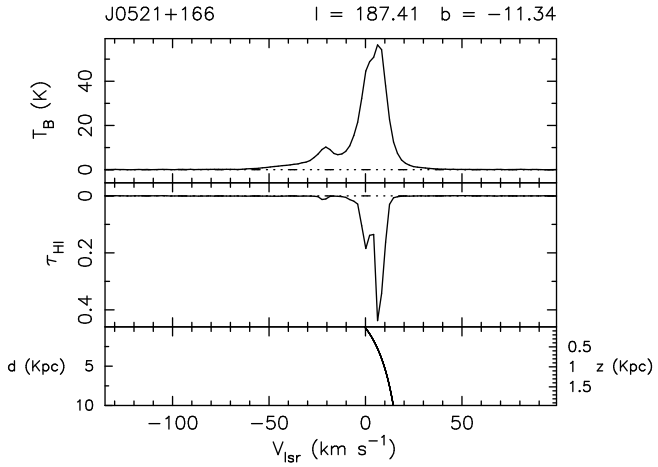

(a)

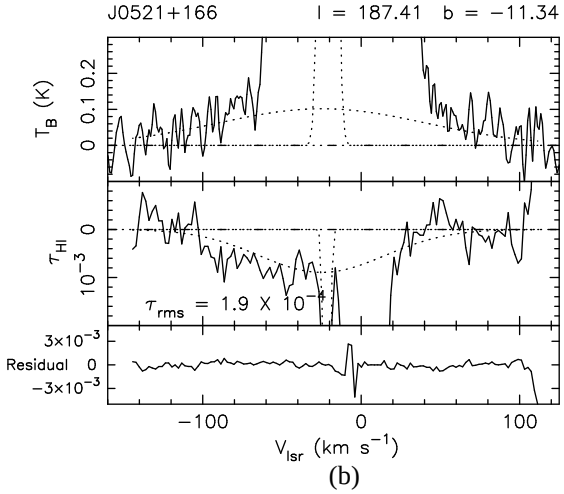

(b)

Fig. 5.2 The HI optical depth spectra from the WSRT towards the source J0521+166 along with the HI brightness temperature profile towards the same line of sight from the Leiden-Dwingeloo survey and the approximate variation of radial component of Galactic differential rotation along the line of sight, as a function of distance (the scale along the left side) and as a function of vertical height (scale on the right side). Figure(b) shows the same HI optical depth and emission profiles, except that the y-axis is magnified to show the very low optical depth features and their HI emission counterparts. The dotted lines are the fitted gaussian models for these features and the lower panel shows the residual in the optical depth spectrum after subtracting the Gaussian model from the observed profile.

Table 5.4 The discrete HI absorption & emission components, identified from the profiles towards the source J0521+166

Absorption (WSRT)			**Emission** (LDS)				
τ_{HI}	V_{lsr} (km s^{-1})	FWHM (km s^{-1})	T_B (K)	V_{lsr} (km s^{-1})	FWHM (km s^{-1})	N_{HI} $\times 10^{20}$ (cm^{-2})	T_S (K)
0.14(0.001)	+9.94(0.01)	2.99(0.03)	—	—	—		
0.44(0.01)	+6.9(0.2)	3.35(0.02)	22.3(0.9)	+7.82(0.04)	6.0(0.1)	2.6	50(4)
0.03(0.003)	+2.1(0.3)	1.5(0.1)	36(1)	+4.1(0.04)	14.9(0.2)	1.0	120(17)
0.16(0.003)	+0.4(0.02)	4.61(0.06)	10.5(0.7)	+0.71(0.03)	4.8(0.1)	0.97	66(5)
0.014(0.0009)	–21.7(0.09)	3.3(0.3)	5.14(0.09)	–20.87(0.05)	7.8(0.2)	7.8	367(32)
—	—	—	5.3(0.1)	–11.2(0.3)	48.3(0.6)	5.0	>5300
0.0009(0.0002)	–24(8)	93(19)	0.10(0.04)	–24(12)	155(36)	3.1	111(89)

spectrum clearly shows four distinct groups of absorption features, clustered in terms of their LSR velocities. One near zero velocity, another extending up to ∼–25 km s^{-1}, a third group centered around ∼–60 km s^{-1} arising in the Perseus arm and a fourth group at beyond ∼–100 km s^{-1} in the outer arm. The spin temperature of all the narrow HI absorption features are ∼100 K, the typical temperatures seen in the cold neutral phase of the Interstellar medium.

5.4.3.1 The low optical depth features Apart from the narrow lines, with the derived spin temperatures in good agreement with the values expected in the CNM, there are two features, with spin temperatures ∼830K and ∼375K (Fig. 5.3.b). This profile is more complicated as compared to the other ones studied here and we cannot rule out the possibility of blending. This possibility is more likely for the HI absorption features centered around –110 km s^{-1} (Fig. 5.3.b). The velocity resolution used for our observations (2.1 km s^{-1}) was unable to separate out the narrow HI absorption components. Even though the HI absorption profile clearly indicate at least three components in that velocity range, gaussian fit was able to obtain only a single component with a width of ∼21 km s^{-1} (Table 5.4). We have also detected an HI absorption component of width ∼31 km s^{-1} centered at –63 km s^{-1}, which coincides with the velocity of the Perseus arm. As we mentioned earlier, if the cold gas as well as warm gas is seen in absorption, then the measured spin temperature of the warm component is only a weak lower limit of the actual value. The widths of these two low optical depth features are 31 km s^{-1} and 21 km s^{-1}. If these widths have a kinematic origin, the thickness of the absorbing layer of HI should be ∼ 2.5 Kpc and 1.8 Kpc, respectively. These values are similar to the thickness of the gas layer associated with spiral arms in the Galaxy.

5.4.4 J2052+365

Figure 5.4.a shows the HI emission and absorption profiles towards this source. This line of sight is close to the previous direction. The two sets of HI absorption features are seen in this case too. However, the outer arm is not seen. Overall, the profile is far less complicated here, as compared to the line of sight towards J2038+513.

5.4.4.1 The low optical depth features Towards J2052+365, there are three features, centered at +27 km s^{-1}, –21 km s^{-1} and –63 km s^{-1} with peak τ_{HI} of 0.004, 0.006 and 0.004 respectively (Fig. 5.4b). Interestingly, none of these three features are seen in HI emission. One possible reason for this is that the corresponding HI emission line brightness temperature being very low, this signal is buried within the HI emission from other features. Assuming a spin temperature of 100K, for an optical depth of 0.004 and a velocity width of 3 km s^{-1} would mean an HI column density of $\sim 2.0 \times 10^{18}$ cm^{-2}. Apart from these three, the rest of the cold HI features along

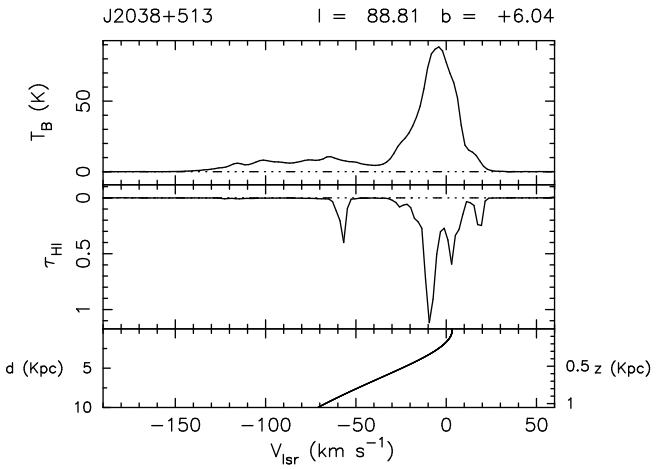

(a)

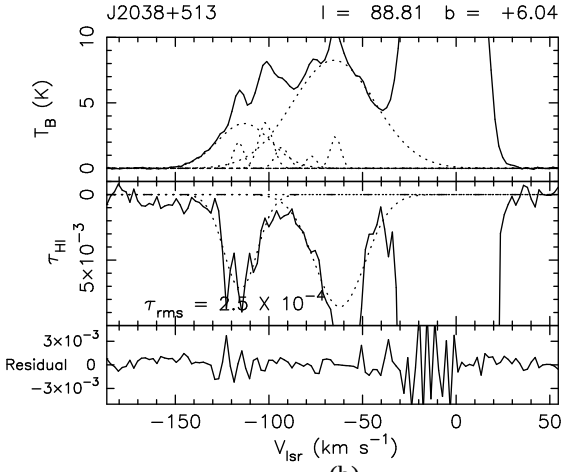

(b)

Fig. 5.3 The HI optical depth spectra from the WSRT towards the source J2038+513 along with the HI brightness temperature profile towards the same line of sight from the Leiden-Dwingeloo survey and the approximate variation of radial component of Galactic differential rotation along the line of sight, as a function of distance (the scale along the left side) and as a function of vertical height (scale on the right side). Figure(b) shows the same HI optical depth and emission profiles, except that the y-axis is magnified to show the very low brightness temperature features in the HI emission profile and the low optical depth features. The dotted lines are the fitted gaussian models for these features and the lower panel shows the residual in the optical depth spectrum after subtracting the Gaussian model from the observed profile.

Table 5.5 The discrete HI absorption & emission components, identified from the profiles towards the source J2038+513. Column 7 lists the HI column density derived from the HI emission data and column 8 shows the calculated spin temperature.

	Absorption (WSRT)		**Emission** (LDS)				
τ_{HI}	V_{lsr} (km s^{-1})	FWHM (km s^{-1})	T_B (K)	V_{lsr} (km s^{-1})	FWHM (km s^{-1})	N_{HI} $\times 10^{20}$ (cm^{-2})	T_S (K)
0.35(0.009)	+18.57(0.02)	3.0(0.2)	—	—	—	—	
0.061(0.006)	+15.0(0.8)	8(1)	9.0(0.4)	+15.9(0.2)	7.6(0.4)	1.3	148(10)
0.36(0.01)	+7.9(fix)	2.34(0.07)					
0.61(0.03)	+3.2(fix)	3.96(0.09)	16.7(0.8)	+5.40(0.07)	5.5(0.2)	1.8	27(3)
0.34(0.01)	–3.6(0.5)	11(2)	89.6(0.3)	–4.7(fix)	19.1(0.3)	33	264(8)
1.37(0.07)	–9.2(fix)	5.29(0.07)	—	—	—	—	
0.24(0.01)	–16.56(0.09)	4.7(0.2)	—	—	—	—	
0.090(0.003)	–24.7(0.2)	7.4(0.4)	15.7(0.6)	–23.8(0.2)	12.7(0.5)	3.8	174(13)
0.94(0.9)	–55(5)	1.2(fix)	—	—	—	—	
0.24(0.02)	–58.4(fix)	5.3(0.2)	—	—	—	—	
0.01(0.002)	–63(2)	31(6)	8.3(0.5)	–65(3)	52(6)	8.3	830(310)
	—	—	2.5(0.5)	–64.4(0.5)	6(2)	0.31	
—	—	—	0.9(0.8)	–77(1)	6(5)	0.12	
—	—	—	1.6(1)	–93(4)	8(7)	0.26	
—	—	—	4(2)	–102(2)	9(5)	0.61	
0.008(0.002)	–115(2)	21(5)	3(2)	–113(9)	33(9)	2.2	375(450)
—	—	—	2.1(0.8)	–116.1(0.7)	6(2)	0.25	

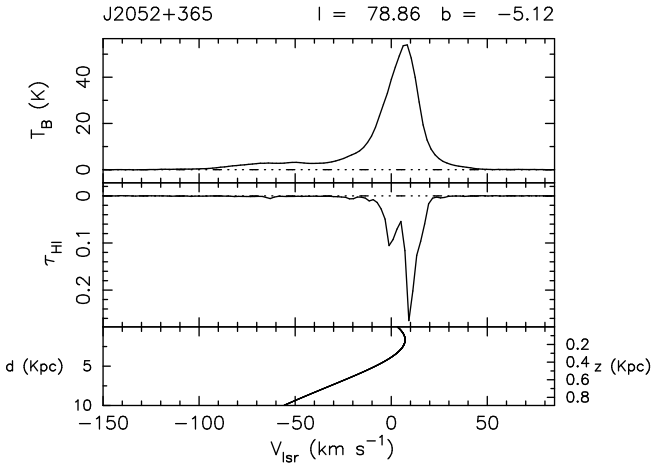

(a)

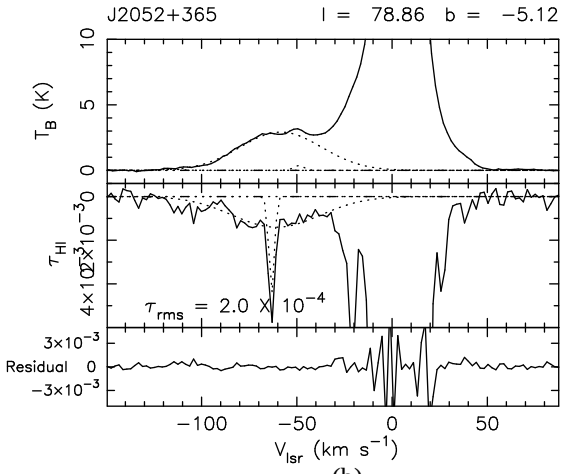

(b)

Fig. 5.4 The HI optical depth spectra from the WSRT towards the source J2052+365 along with the HI brightness temperature profile towards the same line of sight from the Leiden-Dwingeloo survey and the approximate variation of radial component of Galactic differential rotation along the line of sight, as a function of distance (the scale along the left side) and as a function of vertical height (scale on the right side). Figure(b) shows the same HI optical depth and emission profiles, except that the y-axis is magnified to show the very low optical depth features and their HI emission counterparts. The dotted lines are the fitted gaussian models for these features and the lower panel shows the residual in the optical depth spectrum after subtracting the Gaussian model from the observed profile.

Table 5.6 The discrete HI absorption & emission components, identified from the profiles towards the source J2052+365. Column 7 lists the HI column density derived from the HI emission data and column 8 shows the calculated spin temperature.

	Absorption (WSRT)		**Emission** (LDS)				
τ_{HI}	V_{lsr} (km s^{-1})	FWHM (km s^{-1})	T_B (K)	V_{lsr} (km s^{-1})	FWHM (km s^{-1})	N_{HI} $\times 10^{20}$ (cm^{-2})	T_S (K)
—	—	—	0.2(0.1)	+40(1)	5(3)	0.02	
0.004(0.002)	+26.6(0.7)	3(2)	—	—	—	—	
0.14(0.003)	+11.7(0.1)	9.9(0.2)	—	—	—	—	
0.15(0.005)	+9.4(0.04)	3.3(0.1)	38.1(0.8)	+8.6(0.1)	12.1(0.1)	8.9	254(14)
			13.0(0.3)	+0.7(0.2)	39.0(0.6)	9.8	
0.10(0.004)	–0.1(0.1)	6.2(0.3)	16.4(0.8)	–0.9(0.3)	12.9(0.4)	4.1	164(15)
0.01(0.002)	–8(2)	10(3)	—	—	—	—	
0.006(0.001)	–21.2(0.8)	5(2)	—	—	—	—	
			0.38(0.09)	–49.0(0.7)	6(2)	4.6	
0.004(0.002)	–63.3(0.9)	3(2)	—	—	—	—	
0.0014(0.0005)	–60(10)	54(9)	2.9(0.04)	–58.4(0.6)	50(1)	2.8	2071(566)

this line of sight have larger optical depths.

We have detected an HI absorption feature at a mean LSR velocity of ∼–60 km s^{-1} and a peak optical depth of $\sim 1.4 \times 10^{-3}$ (Fig. 5.4.b). The corresponding HI emission feature has a peak T_B ∼2.9 K, centered at ∼–60 km s^{-1} and a FWHM ∼54 km s^{-1}. The estimated spin temperature is ∼2000K (Table 5.4.4). The width of this line and the estimated spin temperature indicate the origin of this feature in the warm neutral medium. However, an HI emission feature, centered near zero velocity, peak line brightness temperature of ∼13K and FWHM ∼39 km s^{-1} was not detected in HI absorption. The reason for this non-detection is clear from Fig. 5.4a. The spread of narrow absorption features over this velocity range has covered the weak absorption arising in the WNM. For this direction, the detected WNM absorption feature is at ∼–60 km s^{-1}, placing it in the Perseus arm of the Galaxy. Therefore the errors in the HI emission line brightness temperature is larger, because the $30^{'}$ beam of the Dwingeloo telescope is sampling larger areas at larger distances from us. Therefore, the measured line brightness temperature can be affected by beam dilution. Using the value of HI line brightness temperature obtained from the Leiden-Dwingeloo survey, we obtained the spin temperature of WNM to be 2071K. Following the calculations by Liszt (2001), we find that **a value for spin temperature ∼2070 K would imply a kinetic temperature of ∼8000K and a number density of ∼0.15 cm^{-3}** if no Ly-α photons are present in the WNM. For a fraction of Ly-α photons > 0.0001 from the early type stars threading the warm gas, our estimate of the spin temperature will demand the WNM to be in the thermally unstable phase (no pressure equilibrium). As in the case of J0502+252, our value for the spin temperature does not agree with the predictions of the McKee-Ostriker model.

5.4.5 J2202+422

Figure 5.5.a shows the HI emission and absorption profiles towards this source. This line of sight is towards l = 92.6° and b = –10.4°. HI absorption was detected only from the local gas, though the HI emission is seen over a wider range of velocities. This source is also known as BLLAC, known for the intrinsic flux density variations. During the time of the present observations, the measured flux density was 2.0 Jy against the quoted value 6.1 Jy in the VLA calibrator manual. Hence, we failed to reach the expected sensitivity levels in HI optical depth.

5.4.5.1 The low optical depth features We have detected HI absorption in the WNM at near zero LSR velocity towards this direction. The peak optical depth is ∼ 0.004 and the brightness temperature is ∼ 5.9K. The spin temperature is found to be ∼1500K, which is below the allowed range of temperatures for the 2 phase model by Wolfire et al (1995), as well as the 3 phase model of McKee & Ostriker (1977). The width of this line is ∼ 31 km s^{-1}, indicating an extent of ∼ 2.2 Kpc along

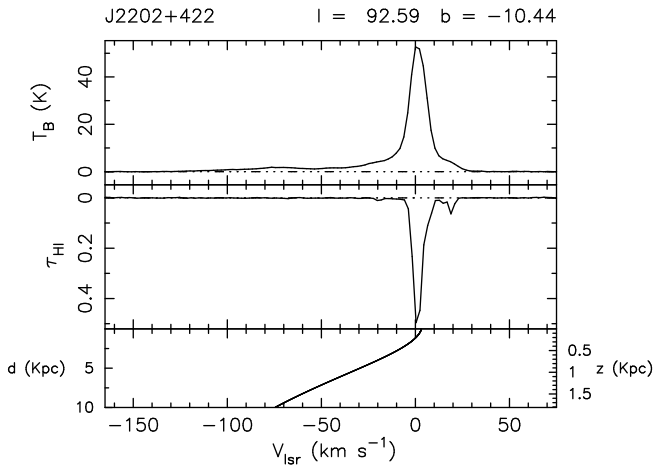

(a)

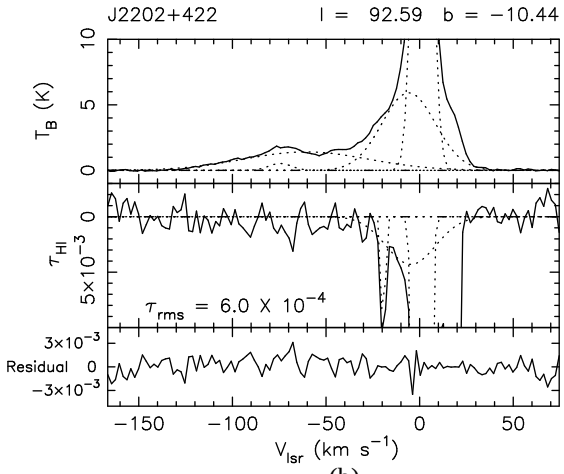

(b)

Fig. 5.5 The HI optical depth spectra from the WSRT towards the source J2202+422 along with the HI brightness temperature profile towards the same line of sight from the Leiden-Dwingeloo survey and the approximate variation of radial component of Galactic differential rotation along the line of sight, as a function of distance (the scale along the left side) and as a function of vertical height (scale on the right side). Figure(b) shows the same HI optical depth and emission profiles, except that the y-axis is magnified to show the very low optical depth features and their HI emission counterparts. The dotted lines are the fitted gaussian models for these features and the lower panel shows the residual in the optical depth spectrum after subtracting the Gaussian model from the observed profile.

Table 5.7 The discrete HI absorption & emission components, identified from the profiles towards the source J2202+422. Column 7 lists the HI column density derived from the HI emission data and column 8 shows the calculated spin temperature.

Absorption (WSRT)			**Emission** (LDS)				
τ_{HI}	V_{lsr} (km s^{-1})	FWHM (km s^{-1})	T_B (K)	V_{lsr} (km s^{-1})	FWHM (km s^{-1})	N_{HI} $\times 10^{20}$ (cm^{-2})	T_S (K)
0.07(0.02)	+19.4(0.7)	3(1)	—	—	—	—	
0.02(0.002)	+15(1)	4(2)	3.0(0.7)	+15.8(0.5)	13(2)	0.76	150(55)
0.088(0.002)	+7.1(0.04)	3.7(0.1)	—	—	—	—	
0.52(0.001)	+1.12(0.007)	5.15(0.02)	48.6(0.5)	+1.50(0.02)	9.79(0.07)	9.2	93(2)
0.011(0.004)	–19.4(0.2)	3(1)	—	—	—	—	
			1.4(0.1)	–61(5)	79(11)	2.1	
			0.5(0.2)	–75(2)	14(5)	0.15	
0.004(0.0007)	–4(3)	31(4)	5.9(0.4)	–6(2)	33(5)	3.9	1475(434)

the line of sight, assuming the width to arise from the kinematics of the absorbing gas.

5.4.6 HI absorption in the Warm neutral medium

As we mentioned earlier, prior to this experiment there were only two detections of HI absorption in the Warm neutral medium (Carilli et al., 1998 & Dwarakanath et al., 2002). Table 5.8 summarizes all the obtained results, including the present work.

5.4.6.1 The location of the absorbing gas The location of the absorbing medium is obtained based on longitude-velocity plots of HI emission from the Leiden-Dwingeloo survey. While there is no obvious correlation between the spin temperature of the WNM and its location, the values of T_S are the highest in the most distant gas (towards Cygnus A) and the lowest for the local arm (towards J2202+422). It is interesting that three out of the five results listed in Table 5.8 are located in the Inter arm regions.

5.4.6.2 The variation of the spin temperature of the WNM From Table 5.8, it is evident that the measured spin temperature of the Intercloud medium spans a large range, from $\sim$1500K to $\sim$ 6000K. HI absorption measurement of WNM in the local arm, Perseus arm, as well as inter arm region are available now. Except for the case of Cygnus A (Carilli et al., 1998), all the other observations has used the Leiden-Dwingeloo survey for the HI emission data to estimate the spin temperature. Given the spatial resolution of $\sim 30^{'}$ for the LDS, the linear scales probed vary from few parsecs in the local gas to $\sim$15 pc in the Perseus arm. Carilli et al., (1998) has listed the WNM HI brightness temperature (T_B) measured using the Effelsberg 100m telescope as well as the LDS (25m Dwingeloo telescope). In the velocity range –67 to –76 km s^{-1}, the T_B measured by the LDS (T_B = 4.7 $\pm$ 2 K) is marginally low as compared to the Effelsberg estimate (5.6 $\pm$ 1 K). If there is structure over a scale of few parsecs in the WNM, then one would expect differences in the values obtained from the Effelsberg and Dwingeloo. Since there is no noticeable difference in the measured HI brightness temperatures, we can assume that gas is uniform over the scales probed by the Dwingeloo survey. Once this assumption is made, table 5.8 would imply a lower spin temperature for the Intercloud medium in the local arm, as compared to the more distant gas. Towards the source J2202+422, the best fit gaussian for the HI absorption in the WNM is centered at $\sim$ 6 km s^{-1} and the estimated spin temperature is $\sim$ 1500K. All other values for the spin temperature of the WNM located at larger distances are higher than this value.

Table 5.8 The HI 21cm-line absorption measurements of the WNM. The second and third columns list the Galactic longitude and latitude of the program sources. The location of the absorbing cloud is obtained based on longitude-velocity plots of HI emission from the Leiden-Dwingeloo survey.

Source	l (deg)	b (deg)	V_{lsr} (km s^{-1})	location	τ_{HI}	FWHM (km s^{-1})	T_S (K)	Comments
Cygnus A	76.19	+5.76	–40 to –36	Inter arm (Local - Perseus)	8.9×10^{-4}	—	4800	Carilli et al., 1998
			–63 to –78	Inter arm (Perseus - Outer)	8.5×10^{-4}	—	6000	
3C 147	161.69	+10.30	–29	Perseus arm	0.0019	54	3600	Dwarakanath et al., 2002
J0502+252	177.73	–9.91	–20	Inter arm (Local - Perseus)	0.0023	59	2478	Present Observations
J2052+365	70.86	–5.12	–60	Perseus arm	0.0014	54	2071	Present Observations
J2202+422	92.59	–10.44	-6	Local gas	0.004	31	1475	Present Observations

5.4.7 HI absorption in the LVD gas

Figs **??** shows the tentative detection of HI absorption in the large velocity dispersion gas, the existence of which was found from the Leiden-Dwingeloo survey by Kalberla et al (1998). At this point we would like to emphasize the difference between the Warm Neutral Medium and the LVD components. HI emission from the WNM is seen at brightness temperatures of a few Kelvins, whereas the LVD features has a peak HI line brightness temperature of $\sim$0.1K. The velocity-width of the WNM HI is less than half that of the LVD gas.

Quite how atomic gas comes to be moving at such high (random) speeds, is hard to understand: why is the gas not ionized by shocks? One explanation is that the LVD component could be composed of a vast number of dense gas clouds which, by virtue of having a high internal pressure, resist shock-compression by the ram pressure of the medium through which they plough. Infact, a number of such models have been suggested in the recent times. A cold gas component in the baryonic dark halo was predicted by Gerhard & Silk (1996). Kalberla et al. (1999) invoked a similar model to explain the γ-ray background emission detected by EGRET. The model of Walker and Wardle (1999) attempts to provide a framework for understanding the broader problem of High Velocity Clouds also. In short, the models predict small, dark, dense molecular clouds distributed throughout the Galactic halo, colliding with each other, ionized by shocks and rendered unbound. In subsequent adiabatic expansion, the collision products may rapidly become very cold and become effective 21cm absorbers. Later, when the density is much lower, weak shocks propagate across the expanding gas and reheat it to a few thousand degrees, making it visible only in 21 cm emission. The predicted velocity dispersion in this model is 55 km s^{-1}, in good agreement with width of the HI emission lines reported by Kalberla et al. (1998).

Almost independent of which physical model of the LVD gas is preferred, the absorbing material is expected to move on trajectories which reach a great distance above the Galactic disk, and the gas should therefore be seen to have a large scale-height. Consequently a significant fraction of the HI mass of the Galaxy might be residing in this population of LVD clouds. The value of spin temperature, T_S $\sim$100K, obtained from our data is very much in agreement with the temperature predicted by various models (For eg., the adiabatically cooling phase in the model by Walker & Wardle, 1999). Towards the other sources observed in this project, either the rms fluctuations in the HI optical depth was not low enough to detect such a feature, or the velocity spread in the Galactic HI features were too large to detect any underlying weak absorption component.

5.5 CONCLUSIONS

In this chapter, we have presented the results of a high sensitivity HI line search for HI absorption in the Warm Neutral medium. These are one of the earliest detections of its kind. Prior to this work there was only two measurements of HI absorption in the WNM. We have added three more detections. We have found evidence for variation of spin temperature in the WNM and the influence of Ly-α radiation field in the value of spin temperature. In addition to this, we have detected HI absorption in the high velocity gas in the Outer arm of the Galaxy. The gas is found to be warm, with a spin temperature of $\sim$450K. We have also detected HI absorption in the large velocity dispersion gas, and estimate its spin temperature to be $\sim$100K. However, this is a marginal detection. If confirmed, this will be the first detection of HI absorption in LVD gas.

REFERENCES

1. Brand, J., Blitz, L., 1993, Astr. Astrophys., 275, 67.
2. Brasken, M., Kyrölä, E., 1998, Astron. Astrophys., 332, 732.
3. Braun, R., Walterbos, R.A.M., 1992, Astrophys. J., 386, 120.
4. Carilli, C.L., Dwarakanath, K.S., Goss, W.M., 1998, Astrophys. J. Lett., 502, L79.
5. Clark, B.G., Radhakrishnan, V., Wilson, R.W., 1962, Astrophys. J., 135, 151.
6. Clark, B.G., 1965, Astrophys. J., 142, 1398.
7. Cox, D.P., Smith, B.W., 1974, Astrophys. J., 189, L105.
8. Dalgarno, A., McCray, R.A., 1972, Ann. Review of Astron. Astrophys., 10, 375.
9. Dickey, J.M., Kulkarni, S.R., Heiles, C.E., van Gorkom, J.H., 1983, Astrophys. J. Suppl., 53, 591.
10. Dwarakanath, K.S., Carilli, C.L., Goss, W.M., 2002, Astrophys. J., 567, 940.
11. Field, G.B., 1959, Astrophys. J., 129, 551.
12. Field, G.B., Goldsmith, D.W., Habing, H.J., 1969, Astrophys. J.Lett., 155, L149.
13. Gerhard, O., Silk, J., 1996 astrophys. J., 472, 34.
14. Hartmann, D., Burton, W. B., 1995, An Atlas of Galactic Neutral Hydrogen, Cambridge Univ. Press.

15. Heiles, C., Troland, T.H., 2002, eprint arXiv:astro-ph/0207104

16. Heiles, C., Troland, T.H., 2002, eprint arXiv:astro-ph/0207105

17. Kalberla, P.M.W., Westphalen, G., Mebold, U., Hartmann, D., Burton, W.B., 1998, Astron. Astrophys. Lett., 332, L61.

18. Kalberla, P. M. W., Shchekinov, Yu. A., Dettmar, R.-J., 1999,

19. Astron. Astrophys. Lett., 350, L9.

20. Liszt, H., 2001, Astron. Astrophys., 371, 698.

21. Mckee, C.F., Ostriker, J.P., 1977, Astrophys. J., 218, 148.

22. Mebold, U., Hills, D. ,1975, Astron. Astrophys., 42, 187.

23. Mebold, U., Winnberg, A., Kalberla, P.M.W., Goss, W.M., 1981, Astron. Astrophys. Suppl., 46, 389.

24. Radhakrishnan, V., Goss, W.M., Murray, J.D., Brooks, J.W., 1972, Astrophys. J. Suppl., 24, 49.

25. Walker, M., Wardle, M., 1999, in Stromlo Workshop on High-Velocity Clouds, ASP conf. Proc., Vol. 166, eds. B.K. Gibson and M.E. Putman, pp. 269.

26. Wolfire, M.G., Hollenbach, D., McKee, C.F., Tielens, A.G.G.M., Bakes, E.L.O., 1995, Astrophys. J., 443, 152.

27. Wouthuysen, S.A., 1952, Astron. J., 57, 31.

A summary of the new results

HI 21cm-line absorption in diffuse clouds which had earlier been detected in optical absorption

- We have carried out sensitive HI 21cm-line absorption observations using the GMRT toward radio sources located at small angular separation from bright O and B stars whose spectra reveal the presence of intervening high random velocity CaII absorbing clouds, hitherto undetected in HI 21cm-line. ***In 5 out of the 14 directions searched, we detect HI 21cm-line absorption features from these clouds.***

- ***These are the first detections of HI absorption from high random velocity clouds.***

- ***The mean optical depth of these detections is $\sim$ 0.09, consistent with absorption arising from the cold neutral medium.***

A high Galactic latitude HI absorption survey

- We have conducted a sensitive high Galactic latitude HI absorption survey using the GMRT to obtain an independent dataset to compare with the existing optical absorption line data.

- ***With a mean rms sensitivity of $\sim$0.003 in HI optical depth, this is the most sensitive HI absorption survey so far.***
- ***We detected approximately 120 absorption features.***
- ***Of these, 13 are at random velocities greater than 15 km s^{-1}.***
- ***We find that the higher random velocity absorptions have smaller optical depths, as suspected by Rajagopal et al. (1998b), however the estimated spin temperatures are similar to that of the standard clouds.***
- ***We find the histogram of radial velocities to have two gaussian components, one with a dispersion $\sim$7 km s^{-1} and the second one with a dispersion $\sim$20 km s^{-1}.***
- ***While the significance of the wider gaussian component is not clear, it is consistent with the recent discovery of a population of HI clouds in the lower Galactic halo.***

Observation towards the Galactic Center and Anticenter

- Early HI 21cm-line absorption measurements towards the Galactic Center using the Parkes interferometer suggested the existence of a low optical depth ($\tau_{peak} \sim 0.3$), broad ($\sigma_v \sim 35$ km s^{-1}) feature centered at zero LSR velocity, and was attributed to a population of high random velocity diffuse HI clouds.
- However, later observations carried out using the WSRT did not confirm this.
- We have made fresh observations to resolve this longstanding and important issue.
- ***We see clear evidence for the presence of a wide HI absorption feature, with a peak optical depth τ_{HI} $\sim$0.31 and a dispersion σ_v $\sim$50 km s^{-1}.***
- ***We conclude that the Westerbork observations failed to detect this feature due to the insufficient bandwidth used in their observations.***
- ***No such feature was detected towards the Galactic Anticenter down to a 3σ limit of 0.006 in optical depth.***

HI absorption in the Intercloud medium

- The intercloud medium, also known as the Warm Neutral Medium (WNM), remains the least understood among the different phases of the interstellar medium.

- The spin temperature of the WNM and its filling factor are important parameters with implications on the models of the ISM, but only two measurements of HI absorption from the WNM exist till date.
- ***We have detected HI 21cm-line absorption in the Warm Neutral Medium of the Galaxy towards 3 more directions. The measured HI optical depth is in the range 0.0014 to 0.004.***
- ***The estimated spin temperature varies from $\sim$2500K $-$ 1400 K. We obtained a lower limit of $\sim$ 5200K towards the fourth line of sight.***
- The spin temperatures derived from our observations agree with the predictions of the two phase models of the ISM.
- ***We have also detected HI absorption in the high velocity gas in the Outer Arm Complex towards one line of sight. The inferred spin temperature is $\sim$ 450K.***
- ***In addition, we have also detected an unusual HI absorption feature ($\tau \sim$ 0.0009), the position and width of which seem to be correlated to a low T_B ($\sim$ 0.1K) wide ($\sigma_v \sim$ 66 km s^{-1}) HI emission feature in the Leiden Dwingeloo Sky survey, which are known as the large velocity dispersion (LVD) HI gas.***
- If confirmed, this will be the first observational evidence for HI absorption in the LVD HI gas, previously seen only in HI emission. The inferred spin temperature is $\sim$ 100 K.